Journal of Hazardous Materials 211–212 (2012) 77–82

Contents lists available at SciVerse ScienceDirect

Journal of Hazardous Materials

journal homepage: www.elsevier.com/locate/jhazmat

Highly stable and efficient Ag/AgCl@TiO_2 photocatalyst: Preparation, characterization, and application in the treatment of aqueous hazardous pollutants

Jian-Feng Guo, Bowen Ma, Anyuan Yin, Kangnian Fan, Wei-Lin Dai *

Department of Chemistry and Shanghai Key Laboratory of Molecular Catalysis and Innovative Materials, Fudan University, Shanghai 200433, PR China

ARTICLE INFO

Article history:
Received 31 May 2011
Received in revised form
24 November 2011
Accepted 24 November 2011
Available online 1 December 2011

Keywords:
Photocatalyst
Visible-light-driven
Surface plasmon resonance
Silver chloride
Water contaminants

ABSTRACT

A new plasmonic photocatalyst of Ag–AgCl@TiO_2 was prepared by deposition–precipitation and photoreduction. This photocatalyst exhibited efficient photocatalytic activity for the degradation of 4-chlorophenol and photoreduction of Cr(VI) ion under visible light irradiation. Its high photocatalytic activity can be attributed to the surface plasmon resonance effect of Ag nanoparticles, which were highly dispersed on the surface of Ag–AgCl@TiO_2. N_2 adsorption and desorption isotherm spectra, X-ray diffraction, X-ray photoelectron spectroscopy, and transmission electron microscopy were used to determine the correlation between the micro-structure and the catalytic properties of the as-prepared photocatalysts.

1. Introduction

Even since the discovery of its ability to split water under ultraviolet (UV) light, titanium dioxide (TiO_2) has been widely considered the most promising photocatalyst in environmental cleanup [1–5]. Due to its wide band gap (3.2 eV for anatase and 3.0 eV for rutile), which nonetheless permits only UV light to be used, the overall efficiency is largely inhibited under sunlight, which consists of 43% visible and only 5% UV fraction [2,6]. Much effort has been devoted to extending its absorption threshold into the visible region. Attempts have included both nonmetal and metal doping, noble metal deposition, and coupling with other semiconductors [7–16]. Modified TiO_2 has exhibited enhanced photocatalytic activity to some extent, but it still cannot meet the requirements of practical, large-scale utilization. Recently, Awazu et al. have proposed the concept of plasmonic photocatalysis, a series of new types of photocatalysts with surface plasmon resonance (SPR) effects [17]. Bi et al. prepared Ag/AgCl core–shell nanowires by in situ oxidation reaction which showed improved photocatalytic activity under visible light irradiation for the decomposition of methyl orange (MO) dye [18]. In studying AgBr/SiO_2 photocatalysts, Kakuta et al. observed that Ag^0 species formed on AgBr in the early stage of the reaction, and AgBr remained undestroyed throughout the photocatalytic process [19]. Hu et al. synthesized Ag/AgBr@TiO_2 by deposition–precipitation for the destruction of azodyes and bacteria under visible light. This compound kept its high photocatalytic activity and stability through five cycles [20]. Wang et al. prepared efficient and stable Ag/AgCl plasmonic photocatalyst by ion exchange for the photodecomposition of MO under visible light, suggesting that electron–hole separation may occur smoothly in the presence of Ag^0 species on the surface of AgCl [21]. Though silver halides have been extensively used as source materials for photographic films based on their photosensitivity, they have seldom been used as photocatalysts because of their instability in sunlight. However, according to previous research, the SPR effect of silver and silver halide makes it feasible to synthesize a new type of active, stable photocatalyst by combining the advantages of silver and silver halide nanoparticles with TiO_2.

Chlorophenols are classified as important soil and water pollutants. They enter water through their wide use as pesticides, herbicides, and wood preservatives. Particularly, 4-chlorophenol (4-CP), a representative of this class, can have serious consequences for human health and the quality of the environment, especially drinking water. In recent years, arrays of industrial activities have been disturbing the geological equilibrium of metal ions

* Corresponding author. Tel.: +86 21 55664678; fax: +86 21 55665572.
E-mail address: wldai@fudan.edu.cn (W.-L. Dai).

0304-3894/$ – see front matter © 2011 Elsevier B.V. All rights reserved.
doi:10.1016/j.jhazmat.2011.11.082

through the release of large quantities of toxic metal ions into the environment. It is well known that Hg(II), Pb(II), Cd(II), Ag(I), Ni(II), and Cr(VI) ions are very toxic and act as the hazardous pollutants among the metal ions present in the environment.

In the present work, nano-sized Ag/AgCl@TiO_2 particles were prepared by deposition–precipitation and photoreduction through a novel one-pot process. The effect of different UV irradiation times on the catalyst has been fully investigated. 4-CP and Cr(VI) ion are chosen as target aqueous hazardous pollutants to evaluate the photocatalytic activity of the as-prepared nano-sized materials.

2. Materials and methods

2.1. Materials

Silver nitrate (Sinopharm Chemical Reagent Co. Ltd. (SCRC)), cetylmethylammonium chloride (CTAC, SCRC), ammonium chromate (SCRC), and 4-CP (SCRC) were of analytical grade and used as received. P25 TiO_2 was purchased from Evonik Degussa company. Other chemicals used were also of analytical or laboratory grade. Deionized water was used for all synthesis and treatment processes.

2.2. Preparation

In a typical synthesis of Ag/AgCl@TiO_2, 0.2 g of commercial Degussa P25 TiO_2 and 0.3 g of CTAC were added to 100 mL of deionized water and the suspension was stirred for 60 min. Then 2.0 mL of 0.1 M $AgNO_3$ was quickly added to the above mixture. During this process, the excessive surfactant CTAC not only adsorbed onto the surface of P25 to limit the number of nucleation sites for AgCl to grow, resulting in homogenously dispersed AgCl, but also induced Cl^- to precipitate Ag^+ in the suspension. The resulting suspension was stirred for 1.0 h and then placed under irradiation of 4×8 W ultraviolet light for the indicated lengths of time. The suspension was filtered, washed with deionized water, and dried at 80 °C for 12 h. Then the gray powder was calcined at 300 °C for 3 h. Depending on the duration of irradiation, the as-prepared catalysts were denoted as Ag–AgCl@TiO_2-*m*, where "*m*" represented 5, 10, 20, and 30 min of photo-reduction, respectively. For comparison, Ag@TiO_2 was synthesized by a similar process without CTAC. Nitrogen-doped N–TiO_2 was also prepared as described previously for comparison [22]. First, 7 wt.% of ammonia aqueous solution was added dropwise to $Ti(SO_4)_2$ aqueous solution to prepare $Ti(OH)_4$ precipitate. After being filtrated and washed with distilled water five times, the precipitate was dispersed into diluted HNO_3 aqueous solution (HNO_3/TiO_2 (mol) = 0.6) at 60 °C with stirring, and the precipitate was peptized and transformed into a transparent sol with a pale blue tint. After being aged at 50 °C, the sol became a gel. Finally, the xerogel powder was obtained by drying the TiO_2 gel at 50 °C followed by grinding.

2.3. Characterization

The XRD patterns of the as-prepared samples (2θ, range from 10° to 70°) were recorded at room temperature with scanning speed of 2° min^{-1} using Cu $K\alpha$ radiation (λ = 0.154 nm) from a 40 kV X-ray source (Bruker D8 Advance). The textural structures were measured by N_2 adsorption at −196 °C with a Micromeritics TriStar ASAP 3000 system. Specific surface areas of the as-prepared samples were measured using the Brunauer–Emmett–Teller (BET) method. Transmission electron micrographs (TEM) were obtained using a JEOL 2011 microscope operating at accelerating voltage of 200 kV. Ultraviolet–visible (UV–vis.) diffuse reflectance spectroscopy was performed using a SHIMADZU UV-2450 instrument with a collection speed of 40 nm min^{-1} using $BaSO_4$ as the reference. X-ray photoelectron spectroscopy (XPS) measurements were performed on a PHI 5000 C ESCA System with Mg $K\alpha$ source operating at 14.0 kV and 25 mA. All the binding energies were referenced to the contaminant C 1s peak at 284.6 eV of the surface of adventitious carbon.

2.4. Photocatalytic experiment

Photocatalytic experiments were performed in a beaker placed under the lamp bracket, containing aqueous suspensions of Cr(VI) (100 mL, 1.0×10^{-3} M) or 4-CP (100 mL, 10 mg L^{-1}) and 50 mg of powdered catalyst. The light source was a 250 W metal halide lamp (Philips) equipped with wavelength cutoff filters for $\lambda \leq 420$ nm and focused on the beaker. Prior to irradiation, the suspensions were stirred in dark for 30 min to establish adsorption desorption equilibrium. After turning on the lamp, 2 mL suspensions were sampled at certain time intervals (5 min) and centrifuged (Shanghai Anting Scientific Instrument Factory, China) at 13,000 rpm for 5 min to remove the photocatalyst particles. The upper clear liquid was analyzed by recording the characteristic absorption peak of 4-CP at 280 nm with a spectrophotometer (721, Shanghai Jing-ying), to calculate the concentrations of the compounds. The determination of Cr(VI) concentration was performed by the 1,5-diphenylcarbazide (DPC) method [23]. In the evaluation of activity for photo-reduction of Cr(VI), 0.2 mM of ethylenediaminetetraacetic acid, disodium (EDTA) was used as sacrificial electron donator.

3. Results and discussion

3.1. Structural properties

The specific surface area of the samples was measured using the BET method with N_2 adsorption and desorption at −196 °C and the typical results are shown in Fig. 1. It is found that there was no obvious difference before and after the deposition of Ag/AgCl on TiO_2. The pore-size distribution was also very similar for these two materials. The BET surface area of P25 TiO_2 was 50 m^2 g^{-1}, while that of Ag/AgCl@TiO_2-20 was 45.6 m^2g^{-1}, which was very similar to that of the parent P25 TiO_2. N_2 adsorption and desorption results indicated that the introduction of Ag/AgCl had little effect on the structural properties on the TiO_2 support. Fig. 2 shows the XRD patterns of the as-prepared catalysts. All the diffraction lines can be indexed as the anatase and rutile TiO_2, cubic phase Ag and cubic phase

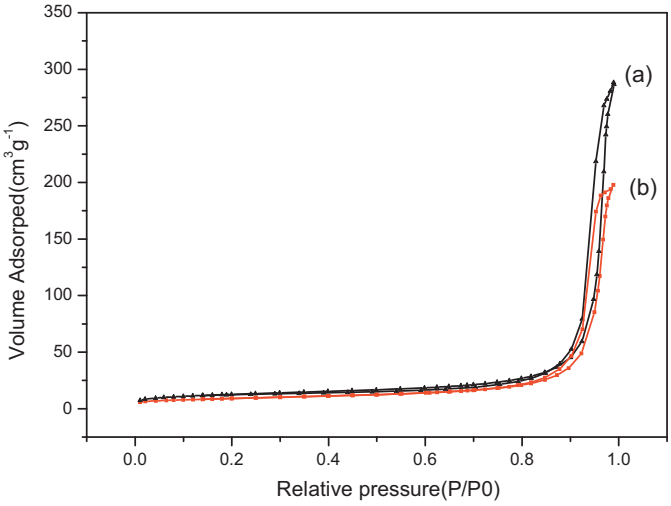

Fig. 1. N_2 adsorption/desorption isotherm of P25 (a) and Ag–AgCl@TiO_2-20 (b).

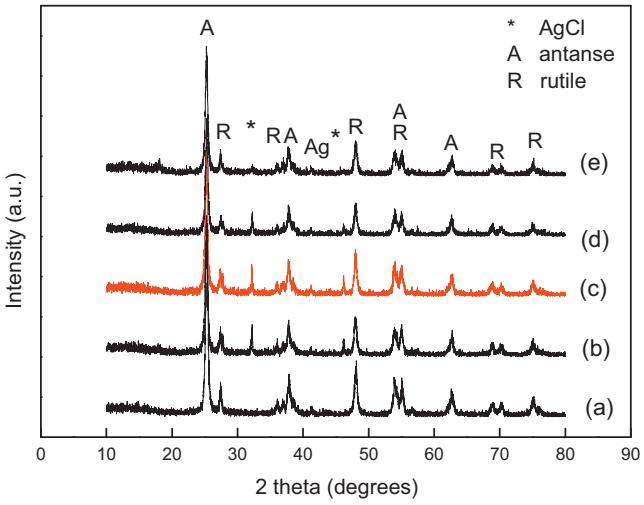

Fig. 2. XRD patterns of Ag–AgCl@TiO_2 with different photo-reduction times (a) P25; (b) Ag–AgCl@TiO_2-5; (c) Ag–AgCl@TiO_2-10; (d) Ag–AgCl@TiO_2-20; and (e) Ag–AgCl@TiO_2-30.

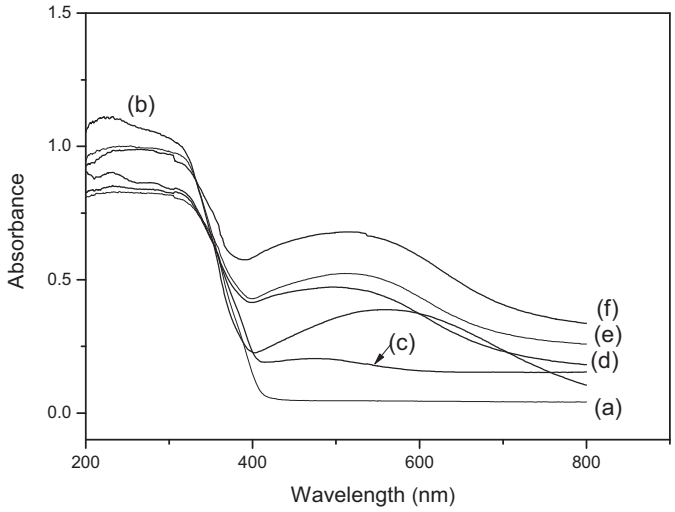

Fig. 4. UV–vis. DRS spectra of Ag–AgCl@TiO_2 for different photo-reduction times (a) P25; (b) Ag/TiO_2; (c) Ag–AgCl@TiO_2-5; (d) Ag–AgCl@TiO_2-10; (e) Ag–AgCl@TiO_2-20 and (f) Ag–AgCl@TiO_2-30.

AgCl, respectively, which are marked clearly in the XRD pattern. As shown, the cubic phase of Ag with lattice constant $a = 4.0861$ Å (JPCDS No. 65-2871) coexists with the cubic phase of AgCl with lattice constant $a = 5.5491$ Å (JPCDS No. 31-1238) in Ag/AgCl@TiO_2. As irradiation time increased, the intensity of peaks ascribed to AgCl decreased, indicating that some AgCl was photo-reduced, and the corresponding Ag nanoparticles were generated on the surface of Ag–AgCl@TiO_2.

3.2. TEM

The TEM images of Ag–AgCl@TiO_2-20 are presented in Fig. 3. Relative to the other catalysts prepared, Ag–AgCl@TiO_2-20 shows the best photocatalytic activity. TEM images of other samples were also taken. However, no obvious changes were observed. Only a single typical sample is shown in this work. Fig. 3 shows that Ag^0 NPs were well dispersed on the surface of Ag–AgCl@TiO_2-20 with diameters ranging from 4 to 5 nm, indicating that the synthesis method reported in the present work was efficient for the preparation of nano-particles with unique particle size distribution. The interlayer spacing $d = 0.23$ nm corresponded to the (1 1 1) plane of cubic Ag (Fig. 3B). Because of the low contrast of AgCl relative to TiO_2 NPs in the TEM images, it cannot be well distinguished from other NPs in the present work.

3.3. UV–vis. diffuse reflectance spectra

Fig. 4 shows the UV–vis. diffuse-reflectance spectra of the as-prepared catalysts. These materials show a strong absorption in the UV region, a characteristic typical of semiconductors. The series of Ag/AgCl@TiO_2 photocatalysts also exhibited broad absorption in the 400–750 nm region of visible light, owing to the surface plasmon resonance of Ag NPs, which were produced by the photo-reduction of AgCl. When the wavelength of the irradiating light is much greater than the diameter of silver NPs, the electromagnetic field across each entire silver NP is essentially uniform. With the oscillations in that electromagnetic field, the weakly bound electrons of the silver nanoparticles respond collectively, giving rise to the plasmonic state. When the incident light frequency matches the plasmonic oscillation frequency, the incident light will be absorbed, resulting in surface plasmon absorption. When the catalysts were irradiated with visible light, some Ag nanoparticles on the surface of the catalysts became larger as a result of the reduction of AgCl (Fig. S3 in Supporting information). Therefore, the shapes and diameters of the Ag NP may vary over a large range. As a result, the frequency of their plasmonic oscillations covers a wide range, permitting Ag/AgCl and Ag/AgCl@TiO_2 to absorb visible and UV light over a wide range [24,25]. As the duration of photo-reduction increased, Ag NP content increased

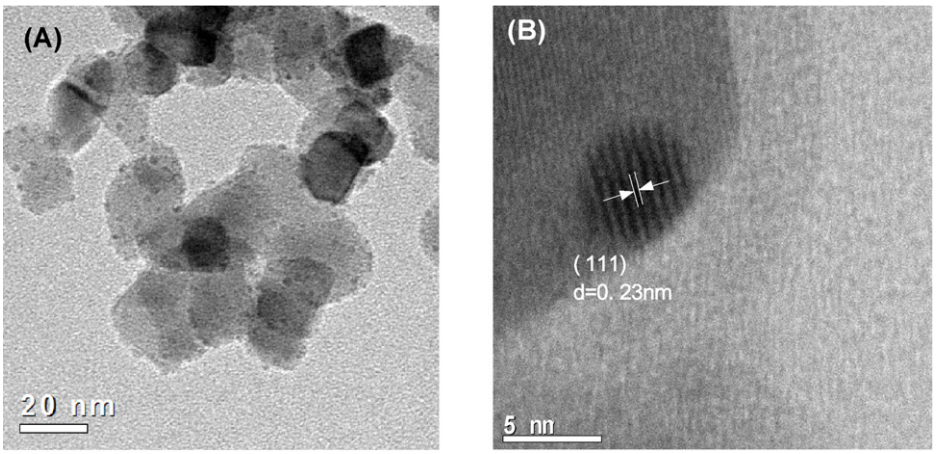

Fig. 3. TEM image of the as-prepared Ag/AgCl@TiO_2-20 photocatalyst.

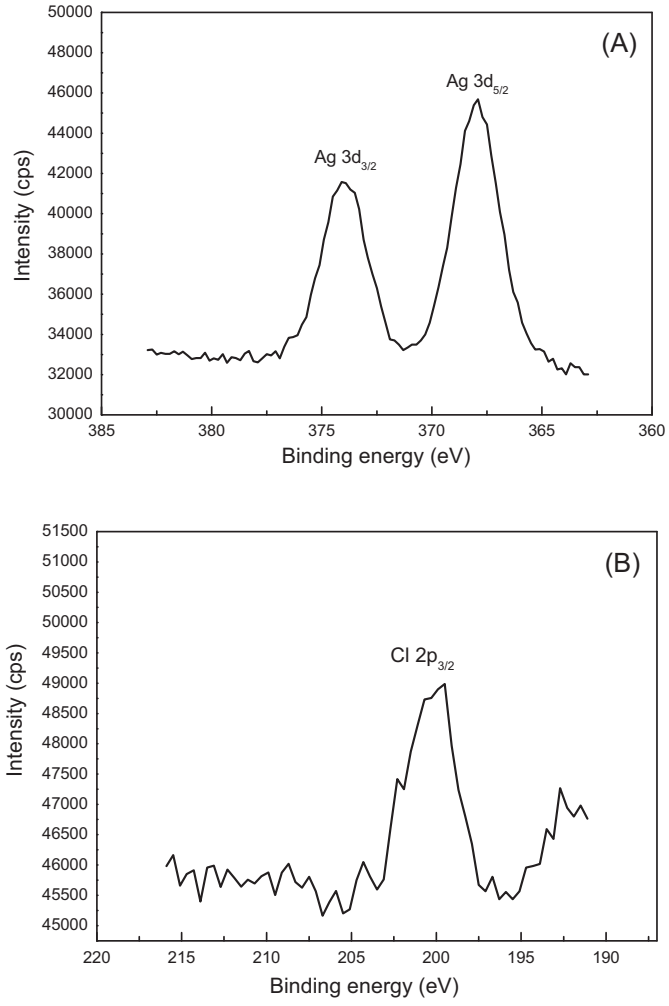

Fig. 5. XPS spectra of Ag–AgCl@TiO_2-20 photocatalyst (a): Ag 3d binding energy and (b): Cl 2p binding energy.

correspondingly, resulting in the enhanced intensity of visible light response from Ag–AgCl@TiO_2-5 to Ag–AgCl@TiO_2-30.

3.4. XPS analysis

Fig. 5 shows the typical XPS spectra of Ag–AgCl@TiO_2-20. Because Ag–AgCl@TiO_2-5, Ag–AgCl@TiO_2-10, and Ag–AgCl@TiO_2-30 have spectra similar to that of Ag–AgCl@TiO_2-20, they are not shown here. In Fig. 5A, the Ag 3d 2/3 XPS peak with binding energy located at 374.9 eV was asymmetric, meaning that Ag existed in at least two valence states. According to the XPS result, the surface atomic ratio of silver to chlorine was 1.4 times higher than the stoichiometric ratio in AgCl (1:1), indicating the existence of excessive Ag on the surface. Considering the fact that there was metallic silver in the as-prepared Ag–AgCl@TiO_2 sample from the XRD, TEM, and XPS results, this implied that the excessive amount of silver might have been produced from the photo-reduction of AgCl on the surface. We calculated the ratios of Ag^0/Ag^+ using the classical chemical analysis method adopted in our previous work (Table 1) [26]. We found that the ratio of Ag^0/Ag^+ increased from 0.40 to 2.65 as the duration of photo-reduction increased from 5 to 30 min. This was consistent well with the XRD results.

3.5. Photocatalytic activity

To evaluate the plasmon-induced photocatalytic activity of Ag–AgCl@TiO_2, the photodegradation of 4-CP and photoreduction

Table 1
Bulk and surface composition of Ag–AgCl@TiO_2 for different photo-reduction times.

Sample	Photoreduction time (min)	Ag content[a] (wt.%)	Ag^0/Ag^+[a]	Ag/Cl[b]
Ag/TiO_2	30	7.9	–	–
Ag–AgCl@TiO_2-5	5	9.8	0.40	1.38
Ag–AgCl@TiO_2-10	10	9.6	1.02	2.05
Ag–AgCl@TiO_2-20	20	9.6	1.40	2.28
Ag–AgCl@TiO_2-30	30	9.5	2.65	3.39

Note:
[a] Data from atomic absorption spectroscopy (AAS).
[b] Molar ratio data from XPS.

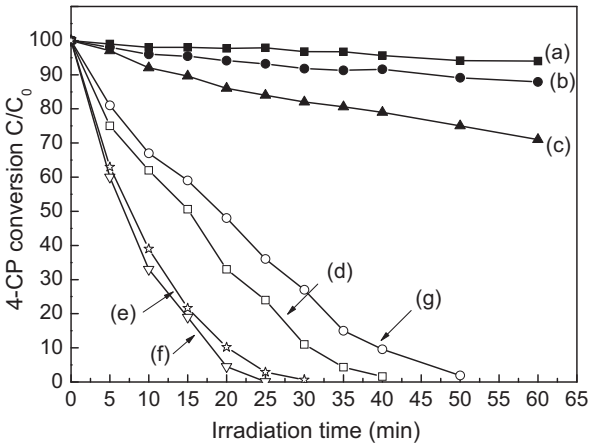

Fig. 6. Photocatalytic activity of Ag–AgCl@TiO_2 for photodegradation 4-CP under visible light irradiation (a) blank; (b) N–TiO_2; (c) Ag/TiO_2; (d) Ag–AgCl@TiO_2-5; (e) Ag–AgCl@TiO_2-10; (f) Ag–AgCl@TiO_2-20; and (g) Ag–AgCl@TiO_2-30.

of Cr(VI) were carried out in aqueous dispersions under visible light irradiation (Figs. 6 and 7). Prior to the activity test of the as-prepared samples, commercial P25 was tested as a reference, and it was found that P25 showed almost no photodegradation activity of 4-CP and Cr(VI) under identical conditions. For comparison, photocatalytic activity evaluations were also performed with Ag/TiO_2 and N–TiO_2 suspensions under identical conditions. Among the three kinds of Ag–AgCl@TiO_2 samples, Ag–AgCl@TiO_2-20 exhibited the most pronounced photocatalytic activity. Regarding the photodegradation of 4-CP, given that the degradation follows a pseudo first order reaction pattern, the degradation rate of 4-CP over Ag–AgCl@TiO_2-5, Ag–AgCl@TiO_2-10, Ag–AgCl@TiO_2-20 , and Ag–AgCl@TiO_2-30 were estimated to be 0.085, 0.095, 0.114,

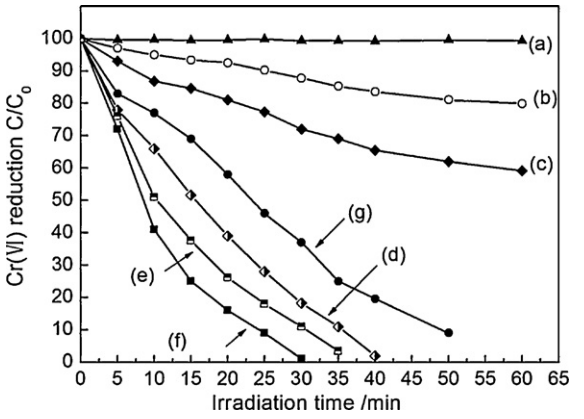

Fig. 7. Photocatalytic activity of Ag–AgCl@TiO_2 for photo-reduction Cr(VI) under visible light irradiation (a) blank; (b) N–TiO_2; (c) Ag/TiO_2; (d) Ag–AgCl@TiO_2-5; (e) Ag–AgCl@TiO_2-10; (f) Ag–AgCl@TiO_2-20 and (g) Ag–AgCl@TiO_2-30.

and 0.057 min^{-1}, respectively, while the degradation rate over Ag/TiO_2 and $N–TiO_2$ were 0.017 and 0.0048 min^{-1}. The rate over $Ag–AgCl@TiO_2$-20 was about 6.8 times faster than that over Ag/TiO_2. As for the photo-reduction of Cr(VI), the results presented in Fig. 7 show the same trend as those from 4-CP. As the duration of photo-reduction increased, the Ag NP content increased correspondingly, changing of the ratios of Ag^0/Ag^+. This has a close connection with photocatalytic activity. There should be an optimum ratio related to the best photoactivity. For a fair comparison of all the $Ag–AgCl/TiO_2$ samples, the ratio of the $Ag–AgCl/TiO_2$-20 sample may best approach the optimum one. That is why the $Ag–AgCl/TiO_2$-30 sample shows lower efficiency in photocatalytic activity.

According to the previous report, during the photo-reduction of Cr(VI), 0.2 mM EDTA was employed as sacrificial electron donator. Without EDTA, the reduction became very slow, which we have demonstrated by our experiment. According to the previous report, in the absence of other organic species, the conjugated oxidation reaction of metal ion reduction is the electrochemical oxidation of water [27]. This is a kinetically slow four-electron process. It can be expected that the addition of sacrificial electron donors may accelerate the photocatalytic reduction of metal ions. As a consequence, photocatalytic reduction in metal/organic photocatalyst systems must be more efficient than in metal photocatalyst systems. In a system in which metal and organic photocatalysts coexisted, organic species accept holes from the valence bands either directly or indirectly, thereby suppressing the electron–hole recombination or increasing reduction efficiency. The result of the present study confirmed the expectation. In this way, the presence of EDTA enhanced the Cr(VI) reduction very effectively. EDTA is known as a strong chelating agent, which may form a stable complex with Cr(VI) and adsorb onto the surface of $Ag–AgCl@TiO_2$ rather than conduct the photocatalytic reduction. To rule out this possibility, physical adsorption of Cr(VI) was conducted in a solution containing 0.2 mM EDTA, the percentage of Cr(VI) removed was observed by dark adsorption and found to be only 12.3% within 1 h.

Puma et al. established a useful method to determine whether the activity of photocatalysts is affected by the radiation absorbed by the catalyst in suspension (because each suspension may absorb photons differently) [28,29]. As shown in Fig. 8, the catalysts $Ag–AgCl@TiO_2$-5, $Ag–AgCl@TiO_2$-10, $Ag–AgCl@TiO_2$-20, and $Ag–AgCl@TiO_2$-30 displayed similar absorption profiles in the aqueous suspensions between the limits of 420 and 800 nm for wavelengths identical to those used in the activity test. Applying the Beer Lambert law, the extinction coefficient as a function of radiation wavelength can be obtained as shown in Supporting information (Fig. S2). Then the average extinction coefficient was estimated by solving the integral (Eq. 12) in Ref. [29] and results are shown in Table 2 [29]. From the data listed in Table 2, it was proved that the average extinction coefficient has no significant relevance to the photocatalytic activity because the Ag/TiO_2 has a much larger average extinction coefficient but a lower photocatalytic activity than the catalyst at $Ag–AgCl@TiO_2$-5, $Ag–AgCl@TiO_2$-10, $Ag–AgCl@TiO_2$-20, and $Ag–AgCl@TiO_2$-30. In the same way, the $Ag–AgCl@TiO_2$-20 sample showed the best photocatalytic activity but a lower average extinction coefficient than $Ag–AgCl@TiO_2$-30. In conclusion, based on the experimental evidence, it was found that results were not affected by the different values of the absorption of radiation realized with each different catalyst (Figs. 6 and 7).

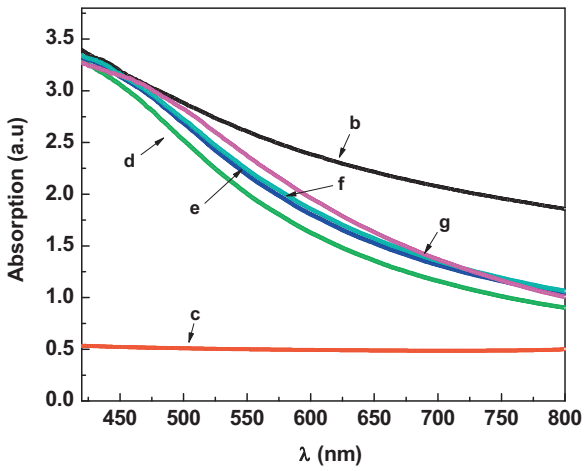

Fig. 8. Absorption of the aqueous suspensions for the catalysts (b) Ag/TiO_2; (c) $N–TiO_2$; (d) $Ag–AgCl@TiO_2$-5; (e) $Ag–AgCl@TiO_2$-10; (f) $Ag–AgCl@TiO_2$-20 and (g) $Ag–AgCl@TiO_2$-30.

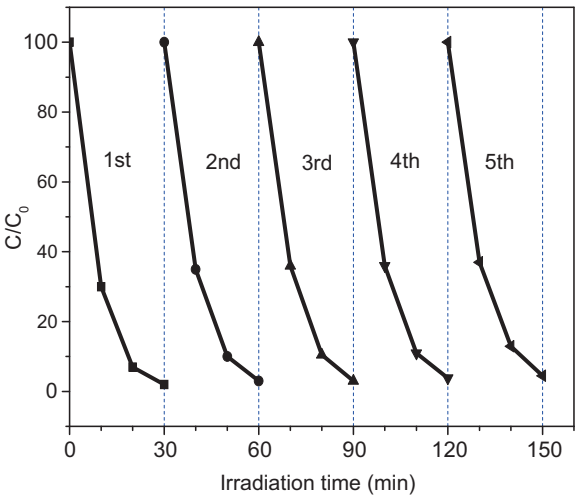

Fig. 9. Irradiation-time dependence of the relative concentration of RhB over $Ag/AgCl@TiO_2$ during repeated photodecomposition experiments under visible light irradiation.

The stability of a practical photocatalyst is as important as its photocatalytic activity. The plasmon photocatalyst $Ag/AgCl@TiO_2$ was here investigated through recycling experiments. As shown in Fig. 9, after five cycles of photodegradation of 4-CP, the sample did not show any significant loss of photocatalytic activity, which indicates that the catalyst can keep stable during the photocatalytic reaction. The XRD pattern of $Ag/AgCl@TiO_2$ after five recycling experiments was almost identical to that of the as-prepared sample (Fig. 10). All the above results indicate that the reported $Ag/AgCl@TiO_2$ is an active and stable visible-light-driven plasmonic catalyst, which may serve as a promising candidate for practical use in the degradation of hazardous pollutants in water.

Table 2
Average extinction coefficients of various catalysts.

Samples	Ag/TiO_2	$N–TiO_2$	$Ag–AgCl\ @TiO_2$-5	$Ag–AgCl\ @TiO_2$-10	$Ag–AgCl\ @TiO_2$-20	$Ag–AgCl\ @TiO_2$-30
κ (L/g cm)	5.27	1.05	3.92	4.23	4.30	4.40

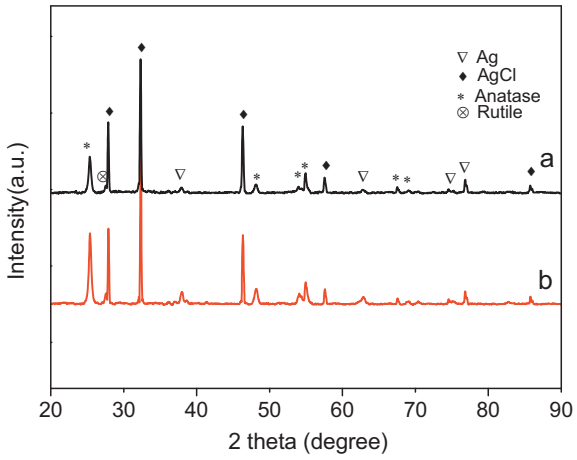

Fig. 10. XRD patterns of the (a) fresh and the (b) reused Ag/AgCl@TiO_2 after 5 cycles.

4. Conclusion

The plasmonic photocatalyst Ag/AgCl@TiO_2 was successfully prepared by one-pot synthesis method. This method is efficient for the photo-degradation of 4-CP and photoreduction of Cr(VI) under visible light irradiation. The effect of photoreduction time of AgCl on the photocatalytic activity has been fully investigated. The ratio of Ag to AgCl was found to influence the photocatalytic activity, and an optimal value was determined. The surface plasmon resonance of Ag NPs, together with the coexistence of Ag and AgCl, played a key role in the enhanced photocatalytic activity. This may help to foster improved understanding and practical use of visible-light-driven plasmonic photocatalysts in the near future.

Acknowledgements

This work is financially supported by NNSFC (Project 21173052 and 20973042), the Research Fund for the Doctoral Program of Higher Education (20090071110011), and the Natural Science Foundation of Shanghai Science & Technology Committee (08DZ2270500).

Appendix A. Supplementary data

Supplementary data associated with this article can be found, in the online version, at doi:10.1016/j.jhazmat.2011.11.082.

References

[1] A. Fujishima, K. Honda, Electrochemical photolysis of water at a semiconductor electrode, Nature 238 (1972) 37–38.
[2] B. O'Regan, M. Graetzel, A low-cost, high-efficiency solar cell based on dye-sensitized colloidal TiO_2 films, Nature 353 (1991) 737–740.
[3] A. Fujishima, L.A. Nagahara, H. Yoshiki, K. Ajito, K. Hashimoto, Thin semiconductor films: photoeffects and new applications, Electrochim. Acta 39 (1994) 1229–1236.
[4] A.P. Davis, D.L. Green, Photocatalytic oxidation of cadmium–EDTA with titanium dioxide, Environ. Sci. Technol. 33 (1999) 609–617.
[5] D.C. Hurum, K.A. Gray, T. Rajh, M.C. Thurnauer, Recombination pathways in the Degussa P25 formulation of TiO_2: surface versus lattice mechanisms, J. Phys. Chem. B 109 (2005) 977–980.
[6] M. Hoffmann, S. Martin, W. Choi, D. Bahnemann, Environmental applications of semiconductor photocatalysis, Chem. Rev. 95 (1995) 69–96.
[7] H.K. Shanmugasundaram Sakthivel, Daylight photocatalysis by carbon-modified titanium dioxide, Angew. Chem. Int. Ed. 42 (2003) 4908–4911.
[8] X. Yang, C. Cao, K. Hohn, L. Erickson, R. Maghirang, D. Hamal, K. Klabunde, Highly visible-light active C- and V-doped TiO_2 for degradation of acetaldehyde, J. Catal. 252 (2007) 296–302.
[9] M. Lim, Y. Zhou, B. Wood, Y. Guo, L. Wang, V. Rudolph, G. Lu, Fluorine and carbon codoped macroporous titania microspheres: highly effective photocatalyst for the destruction of airborne styrene under visible light, J. Phys. Chem. C 112 (2008) 19655–19661.
[10] X. Yang, C. Cao, L. Erickson, K. Hohn, R. Maghirang, K. Klabunde, Synthesis of visible-light-active TiO_2-based photocatalysts by carbon and nitrogen doping, J. Catal. 260 (2008) 128–133.
[11] S. Yamazaki, N. Fujinaga, K. Araki, Effect of sulfate ions for sol–gel synthesis of titania photocatalyst, Appl. Catal. A 210 (2001) 97–102.
[12] F.B. Li, X.Z. Li, Photocatalytic properties of gold/gold ion-modified titanium dioxide for wastewater treatment, Appl. Catal. A 228 (2002) 15–27.
[13] A. Dawson, P.V. Kamat, Semiconductor–metal nanocomposites. Photoinduced fusion and photocatalysis of gold-capped TiO_2 (TiO_2/Gold) nanoparticles, J. Phys. Chem. B 105 (2001) 960–966.
[14] J. Cao, J. Sun, H. Li, J. Hong, M. Wang, A facile room-temperature chemical reduction method to TiO_2@CdS core/sheath heterostructure nanowires, J. Mater. Chem. 14 (2004) 1203–1206.
[15] Q. Zhang, W. Fan, L. Gao, Anatase TiO_2 nanoparticles immobilized on ZnO tetrapods as a highly efficient and easily recyclable photocatalyst, Appl. Catal. B 76 (2007) 168–173.
[16] Y. Zhiyong, M. Bensimon, V. Sarria, I. Stolitchnov, W. Jardim, D. Laub, E. Mielczarski, J. Mielczarski, L. Kiwi-Minsker, J. Kiwi, $ZnSO_4$–TiO_2 doped catalyst with higher activity in photocatalytic processes, Appl. Catal. B 76 (2007) 185–195.
[17] K. Awazu, M. Fujimaki, C. Rockstuhl, J. Tominaga, H. Murakami, Y. Ohki, N. Yoshida, T. Watanabe, A plasmonic photocatalyst consisting of silver nanoparticles embedded in titanium dioxide, J. Am. Chem. Soc. 130 (2008) 1676–1680.
[18] Y. Bi, J. Ye, In situ oxidation synthesis of Ag/AgCl core–shell nanowires and their photocatalytic properties, Chem. Commun. 2009 (2009) 6551–6553.
[19] N. Kakuta, N. Goto, H. Ohkita, T. Mizushima, Silver bromide as a photocatalyst for hydrogen generation from CH_3OH/H_2O solution, J. Phys. Chem. B 103 (1999) 5917–5919.
[20] C. Hu, Y. Lan, J. Qu, X. Hu, A. Wang, Ag/AgBr/TiO_2 visible light photocatalyst for destruction of azodyes and bacteria, J. Phys. Chem. B 110 (2006) 4066–4072.
[21] P. Wang, B. Huang, X. Qin, X. Zhang, Y. Dai, J. Wei, M.H. Whangbo, Ag@AgCl: a highly efficient and stable photocatalyst active under visible light, Angew. Chem. Int. Ed. 47 (2008) 7931–7933.
[22] X. Fang, Z. Zhang, Q. Chen, H. Ji, X. Gao, Dependence of nitrogen doping on TiO_2 precursor annealed under NH_3 flow, J. Solid State Electrochem. 180 (2007) 1325–1332.
[23] P.R. Wittbrodt, C.D. Palmer, Reduction of Cr (VI) in the presence of excess soil fulvic acid, Environ. Sci. Technol. 29 (1995) 255–263.
[24] P. Wang, B. Huang, X. Zhang, X. Qin, H. Jin, Y. Dai, Z. Wang, J. Wei, J. Zhan, S. Wang, Highly efficient visible-light plasmonic photocatalyst Ag@ AgBr, Chem. Eur. J. 15 (2009) 1821–1824.
[25] P. Jain, W. Huang, M. El-Sayed, On the universal scaling behavior of the distance decay of plasmon coupling in metal nanoparticle pairs: a plasmon ruler equation, Nano Lett. 7 (2007) 2080–2088.
[26] J.F. Guo, B. Ma, A. Yin, K. Fan, W.L. Dai, Photodegradation of rhodamine B and 4-chlorophenol using plasmonic photocatalyst of Ag–AgI/Fe_3O_4@SiO_2 magnetic nanoparticle under visible light irradiation, Appl. Catal. B 101 (2011) 580–586.
[27] J.A. Navío, G. Colón, M. Trillas, J. Peral, X. Dom nech, J.J. Testa, J. Padrón, D. Rodríguez, M.I. Litter, Heterogeneous photocatalytic reactions of nitrite oxidation and Cr (VI) reduction on iron-doped titania prepared by the wet impregnation method, Appl. Catal. B 16 (1998) 187–196.
[28] G. Li Puma, J.N. Khor, A. Brucato, Modeling of an annular photocatalytic reactor for water purification: oxidation of pesticides, Environ. Sci. Technol. 38 (2004) 3737–3745.
[29] G. Li Puma, V. Puddu, H.K. Tsang, A. Gora, B. Toepfer, Photocatalytic oxidation of multicomponent mixtures of estrogens (estrone (E1), 17β-estradiol (E2), 17α-ethynylestradiol (EE2) and estriol (E3)) under UVA and UVC radiation: photon absorption, quantum yields and rate constants independent of photon absorption, Appl. Catal. B 99 (2010) 388–397.